Int. Journal of Refractory Metals and Hard Materials 47 (2014) 49–53

Contents lists available at ScienceDirect

Int. Journal of Refractory Metals and Hard Materials

journal homepage: www.elsevier.com/locate/IJRMHM

Formation and densification behavior of reaction sintered alumina–20 wt.% aluminium titanate nano-composites

M. Sobhani *, T. Ebadzadeh, M.R. Rahimipour

Ceramic Department of Materials and Energy Research Center, Alborz, Iran

ARTICLE INFO

Article history:
Received 27 April 2014
Accepted 24 June 2014
Available online 1 July 2014

Keywords:
Alumina/aluminium titanate
Thermal expansion
Reaction sintering
Composites

ABSTRACT

Densification and reaction sintering behavior of the alumina–20 wt.% aluminium titanate nano-composites were studied. Nano TiO_2 powders were used in achieving the aluminium titanate phase during reaction sintering of alumina and titania. High resolution X-ray diffraction (HR-XRD) and scanning electron microscopy (SEM) results revealed that the aluminium titanate formation was affected by heating rate and soaking time at the elevated temperatures. The content of aluminium titanate phase decreased during increment of heating rate and increased during increment of soaking time at sintering temperature. Final densities of the sintered composites at 1550 °C were lower than those sintered at 1450 °C which can be explained by the grain cracking phenomenon induced by thermal expansion mismatch. The residual strain of the aluminium titanate grains released after grain cracking. The Al_2TiO_5 grains cracked along the (010) crystallographic planes because of the most positive expansion of the b-axis, and the lattice parameter b reverted to its original value after grain cracking.

Introduction

Alumina as an industrial ceramics is widely used due to its attractive properties. Strength, melting point, hardness and Young's modulus of alumina are higher than most well known ceramics. Aluminium titanate (Al_2TiO_5) as a second phase in alumina ceramics, with lower Young's modulus and thermal expansion coefficient than the alumina, can therefore enhance the composite's toughness and resistance to thermal shock [1–4]. Additionally, the limited solution of titania can improve the densification of alumina [5,6]. The alumina/aluminium titanate (A/AT) composites can be fabricated by direct mixing of alumina and aluminium titanate (tialite) powders or by in-situ reaction sintering of mixed alumina and TiO_2 powders. In spite of its low thermal expansion coefficient ($\sim 1 \times 10^{-6}$ °C^{-1} for polycrystalline bodies), tialite similar to other pseudobrookite materials exhibits high thermal expansion anisotropy (TEA) ($\alpha_a \approx 11$, $\alpha_b \approx 21$, $\alpha_c \approx -3 \times 10^{-6}$ °C^{-1}) [7–9]. Accordingly, thermal stresses induced during cooling from the sintering temperature in bulk can lead to spontaneous microcracking phenomenon. At the first time, Kuszyk and Bradt [10] proposed that an energy criterion controls the formation of microcracks in ceramics with high thermal expansion anisotropy. They introduce a basic relation between the critical grain size needed for spontaneous microcracking and energy criterion (strain and fracture surface energy). Afterwards, Cleveland and Bradt [11] offer the following developed equation:

$$D_{gr} = \frac{14.4\gamma_f}{E(\Delta T \Delta\alpha_{\max})^2} \tag{1}$$

where γ_f is the fracture surface energy, E is the Young's modulus and $\Delta\alpha_{max}$ is the maximum difference of the thermal expansion coefficients along the crystallographic axes and ΔT is the difference between sintering and room temperatures. The estimated grain size of tialite for microcraking is about 2 μm. Therefore, the size controlling of aluminium titanate phase is the main problem, because the widespread occurrence of microcracking in coarser microstructure, resulting from thermal expansion anisotropy, decreases the mechanical properties. Lawn et al. and Padture et al. [2,3] studies showed that the R-curve behavior in fracture toughness of A/AT composites was a result of aluminium titanate grains bridging during crack propagation. Also Bueno et al. [12] reported the change of toughening mechanism from crack bridging to microcracking in A/20AT composite at the presence of sub-micrometric aluminium titanate particles. Additionally, the physical properties such as the final bulk density of monolithic aluminium titanate at room temperature can be affected by the enlarged aluminium titanate grains. The density degradation due to microcracking (obtained during cooling from the sintering temperature) is accompanied by increased grain size due to rising sintering temperature. The crack volume induced by such microcracking is proportional to $D_{gr}^{0.5}$ [13]. In view of the above, the investigation of microcracking effect on physical properties of

---

* Corresponding author. Tel.: +98 9155022379; fax: +98 2636204139.
E-mail address: manoochehrsobhani@gmail.com (M. Sobhani).

http://dx.doi.org/10.1016/j.ijrmhm.2014.06.018

A/AT composites has drawn little attention. Therefore, in the present work, the effect of different heat treatment schedules on formation and densification of A/20AT composite was investigated. Furthermore, high resolution X-ray diffraction was used to investigate the lattice parameter changes of Al_2TiO_5 during grain cracking caused be thermal expansion anisotropy.

Experimental procedures

The starting materials were α-Al_2O_3 (MR70 average particle size of 0.7 μm), nanosized TiO_2 powder (P25, Degussa-Evonik, Germany) with an average primary particle size of 40 nm. Fig. 1 shows the morphology of the raw materials. A mixture of alumina (≈91.2 wt.%) and titania (≈8.8 wt.%) was used to achieve the sintered A–20 wt.% AT composites. The mixture of desired powders milled in ethanol, using a planetary ball mill with zirconia cup and balls (during 1 h at 250 rpm). Drying was carried out using a hot-plate, while stirring continuously. Afterwards, the powders were grounded in an alumina mortar and sieved. Green specimens, 25 × 5 × 4 mm, were fabricated by uniaxially pressing at 50 MPa. Removal of any defects associated with die pressing was achieved by subsequent wet bag isostatic pressing at 175 MPa. A green density of about 60% of the theoretical limit was obtained using this method. The green bars were sintered using two heat treatment schedules. The first contains preheating at 1100 °C before sintering and the second only contains sintering schedules (listed in Table 1). Densities were determined by the Archimedes's method in deionized water (European Standard EN1389:2003) and theoretical densities were calculated by taking values of 3.99 g cm^{-3} for alumina (ASTM 42-1468), 4.25 g cm^{-3} for rutile (ASTM 21-1276) and 3.70 g cm^{-3} for aluminium titanate (ASTM 26-0040). The strength of sintered bars were measured using three point bending test supported with a span length of 15 mm and cross-head speed of 0.5 mm/min^{-1}. At least five specimens were tested to obtain the average value along with its standard deviation for density and strength measurements. Simultaneous thermal analysis (STA) with differential scanning calorimetry (DSC) and thermo-gravimetric (TG) curves was carried out by a NETZSCH STA 409 PC/PG instrument in air atmosphere with a temperature rising rate from 5 °C/min up to 1400 °C. High resolution X-ray diffraction (HR-XRD) of the composites was determined by X-ray diffraction (Model: Siemens D-500, Germany) using CuK_α ($\lambda = 1.54$ Å) radiation. The HR-XRD data were obtained using $d\theta = 0.005°$ and $t = 2$ s. The parameters for the zero-point shift were refined using standard sample (silicon) diffraction lines. The results were compared with the ASTM Files (for β-aluminium titanate, corundum and rutile [14–16]). Microstructure characterization on polished (1 μm) and thermally etched (100 °C below the sintering temperature during 20 min) surfaces was performed by a TESCAN field emission scanning electron microscopy (FESEM, model MIRA II).

Table 1
Different sintering conditions and determined phases for A/20AT composites.

Sample	Heat treatment schedule	Phases
a	4 h at 1100 °C–2 h at 1450 °C (3 °C/min)	A + AT + R
b	4 h at 1100 °C–2 h at 1500 °C (3 °C/min)	A + AT
c	4 h at 1100 °C–2 h at 1550 °C (3 °C/min)	A + AT
d	2 h at 1450 °C (5 °C/min)	A + AT + R
e	2 h at 1500 °C (5 °C/min)	A + AT + R
f	4 h at 1450 °C (5 °C/min)	A + AT

Results and discussions

Phase development and microstructure studies

The results of DSC and TG analysis of A–20 wt.% AT composite powders are presented in Fig. 2. The endothermic peak at about 90 °C in DSC curve indicates the removal of moisture. Another endothermic peak at 1309 °C is a characteristic peak of aluminium titanate formation during chemical reaction of Al_2O_3 and TiO_2. Considering the Eq. (2) the formation temperature of Al_2TiO_5 in this study is much close to the thermodynamically value due to the high reactivity of the nano TiO_2 powders, in comparison with the previous reports [17–19]. The total mass reduction value in TG curve (−2.66%) is attributed to moisture evaporation. Fig. 3 demonstrates X-ray diffraction patterns of the alumina–20 wt.% aluminium titanate composites sintered at different temperatures listed in Table 1 (samples a, b and c). Considering the molar free energy equation of Al_2TiO_5 formation, the reaction of alumina and titania leads to the formation of aluminium titanate at above 1280 °C [20]:

$$Al_2O_3(\alpha) + TiO_2(\text{Rutile}) \rightarrow Al_2TiO_5(\beta), \Delta G^\circ = 17,000\text{–}10.95\ T(\text{j/mol}). \tag{2}$$

Also it can be noted that the formation of β-Al_2TiO_5 and its solid solution compounds with MgO ($Mg_xAl_{2(1-x)}Ti_{(1+x)}O_5$) using the chemical process can occur at the lower temperatures [21,22]. However, for sample (a) the reaction did not completely happen and the characteristic peak of rutile at $2\theta = 27.44°$ can be observed. Therefore, according to XRD results unreacted titania still remains in sample (a) and formation of aluminium titanate completed after sintering at 1500 °C with a

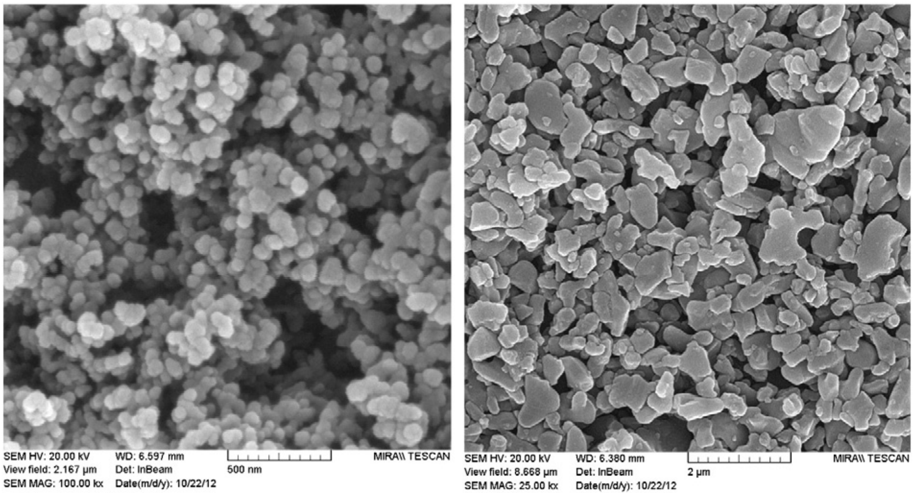

Fig. 1. SEM micrographs of raw materials: alumina (right), nano TiO_2 (left).